

Scientific section: NEOPLASIA

title: Generation of a potent recombinant homophilic chimeric anti-CD20 antibody

authors: Heinz Kohler,<sup>1</sup> Jean D. Amick,<sup>1</sup> Kyle Rector,<sup>1</sup> and Mike Russ<sup>1</sup>

affiliation: <sup>1</sup>Innexus Biotechnology, Incorporated, Coldstream Laboratory, Lexington, KY 40511

Corresponding author: Heinz Kohler

Innexus Biotechnology, Inc.

1501 Bull Lea Rd.

Lexington, KY 40511

email: [hkohler@ixsbio.com](mailto:hkohler@ixsbio.com)

phone: (859)277-9404

fax: (859)514-4959

Abstract word count: 147

Text word count: 3400

Submitted [6/26/2007]; accepted []. Prepublished online as *Blood* First Edition Paper, []; DOI 10.1182/blood-YYYY-MM-NNNNNN.

The online version of the article contains a data supplement.

## **Abstract**

Previously, we have affinity cross-linked a homophilic peptide to antibodies, demonstrating increased potency of antibody conjugates in targeting, apoptosis, and growth inhibition *in vitro*. Here, we describe construction of a chimeric fusion gene derived from the murine anti-CD20 antibody (1F5) variable region, with an engineered homophilic domain at the C-terminus of the human IgG1 sequence. The construct was expressed in CHO suspension cells, and purified. The potency of the homophilic anti-CD20 antibody was compared to a chimeric antibody without the engineered homophilic domain. In this comparison, the homophilic anti-CD20 antibody showed increased binding to a human CD20<sup>+</sup> cell line, and significantly more ADCC, CDC, and induction of apoptosis in three cell lines. In addition, the homophilic anti-CD20 antibody demonstrated increased inhibition of proliferation of two cell lines. These data suggest that engineering a dynamically cross-linking fusion protein is a viable strategy for developing next generation therapeutic antibodies.

## Introduction

For therapeutic application of antibodies, potency is a decisive factor, which affects the therapeutic response in patients undergoing immune therapy. Significant efforts have been made to augment the therapeutic potency of antibodies by increasing the affinity for the target <sup>1</sup>, as well as modifying carbohydrate <sup>2,3</sup> and Fc effector binding sites (<sup>4,5</sup>and refs therein). However, there are practical limits to how much affinity can be improved <sup>6-8</sup>. High-affinity antibodies may be less effective than medium-affinity antibodies, because high affinity antibodies exhibit a decreased rate of diffusion <sup>9</sup>, and affinity is not predictive of anti-proliferative activity <sup>10</sup>. Classical mechanisms invoked in therapeutic potency are CDC, ADCC, and blockage of growth receptors. Induction of apoptosis has recently been recognized as an important mechanism of tumor killing <sup>11,12</sup>. Apoptosis is initiated by cross-linking of receptors that trigger apoptotic signaling pathways <sup>11,12</sup>. For example, Vitteta et al have made chemically cross-linked dimers of anti-CD20 and anti-CD19 antibodies, and have shown that these dimerized antibodies are superior *in vitro* and *in vivo* when compared to the monomeric forms <sup>13</sup>. Other chemical and immunological techniques producing polyvalent antibodies have produced similar potency enhancement <sup>14</sup>, or as a tetravalent F(ab')<sub>2</sub> <sup>15</sup>.

Our laboratory has developed a method that produces dimerizing antibodies and has shown that they possess significantly higher potency *in vitro* and *in vivo*, targeting human and mouse tumors <sup>16,17</sup>. Homophilic antibodies, naturally occurring or engineered, are in equilibrium between monomeric and multimeric forms. In solution, homophilic antibodies behave as monomeric structures, but after attachment to a target, they exert their homophilic potential <sup>18</sup>. We have termed such homophilic antibodies Dynamic Cross-Linking (DXL™) antibodies. This mechanism has several biological implications. First, it increases the density of antibodies on its target, an important parameter for Fc-mediated mechanisms. Second, DXL antibodies can induce targeted receptor cross-linking, a mechanism known to induce apoptosis. Third, induced receptor cross-linking can lead to uptake and internalization of the antibody-receptor complex. All three mechanisms may affect the therapeutic potency of antibodies <sup>19</sup>.

Previously, we have generated such DXL antibodies with improved potency using a photo-chemical affinity cross-linking method. This technology is based on the discovery of affinity sites on antibodies that can be used to photo cross-link peptides. The method used a simple but effective technique by which a peptide of interest can be added to antibodies <sup>20</sup>. One

peptide, which is derived from naturally occurring, self-binding T15 antibodies<sup>21-23</sup>, confers homophilic properties to virtually any antibody. Although chemical modification has proven very effective, it presents a challenge for large-scale production of therapeutic antibodies. For this reason, we have employed molecular biological techniques to generate recombinant DXL antibodies to satisfy the requirements for production, quality control, and FDA requirements.

Given the success of Rituxan™ in treating non Hodgkin's lymphoma (NHL) and recent approval for use in rheumatoid arthritis, we have chosen as a therapeutic target CD20, which is an important B-cell marker, since it is present at high levels in various B-cell cancers, but is undetectable in precursor and plasma B-cells<sup>24</sup>. In this report, we compare the potencies of an anti-CD20 chimeric antibody with a DXL chimeric version. The recombinant antibodies are derived from the mouse anti-CD20 1F5 antibody, with the homophilic DXL peptide located in-frame with the C-terminus of the heavy chain. We demonstrate that the addition of DXL at this location provides a significant improvement in effector functions versus the chimeric antibody without the homophilic domain.

## **Materials and Methods**

### **Cell lines**

JOK-1 cells were a gift of Affimed Inc. JOK-1 cells were grown in RPMI-1640 with Glutamax (Gibco), supplemented with 10% FBS-Premium-HI (Aiken Biologicals), and 1% Penicillin/Streptomycin (Gibco). 1F5 hybridoma, Raji, and Ramos, cells were obtained from the American Type Culture Collection (ATCC), numbers HB-9645, CCL-86, CRL-1596, and TIB-152, respectively. Raji and Ramos cells were maintained in RPMI-1640 Medium with HEPES (ATCC), supplemented with 10% FBS-Premium-HI (Aiken Biologicals), and 1% Penicillin/Streptomycin (Gibco). 1F5 cells were maintained in RPMI-1640 Medium with HEPES (ATCC), supplemented with 10% FBS-low-IgG (Gibco), 1% Penicillin/Streptomycin (Gibco), and 0.5% Glutamax (Gibco). CHO-S cells were purchased from Invitrogen, and were grown in CD CHO medium, supplemented with 1% HT supplement (Gibco), 2% Glutamax (Gibco), and 100 U/ml pen/strep (Gibco). After introduction of vector DNA, CHO-S cells were grown as above with the addition of 1.2 mg/ml G418 (Invivogen) for selection. All cells were maintained at 37°C and 5% CO<sub>2</sub>.

### **Construction of chimeric antibody genes**

Total RNA was isolated from  $\sim 7 \times 10^6$  1F5 hybridoma cells using an RNeasy kit (Qiagen) according to the manufacturer's instructions. First strand cDNA synthesis, cDNA amplification by Long-Distance PCR (LD-PCR), and Proteinase K digestion were carried out using the materials and protocol of the Creator SMART cDNA library kit (Clontech). The 1F5 heavy chain variable regions were amplified from the cDNA pool by PCR using primers modVH1F5fwd and modVH1F5rev. Oligo DNA sequences are provided in Supplemental Figure 1 on the *Blood* website. See the Supplemental Data Set link at the top of the online article. All oligos were purchased from Operon. The 1F5 light chain variable regions were amplified from the cDNA pool by PCR using primers modVL1F5fwd and modVL1F5rev. The heavy chain and light chain PCR products were cloned into the XhoI-NheI and SacI-HindIII sites, respectively, of vector pAc-k-CH3 (Progen Biotechnik GmbH), to form pAc-k-1F5H and pAc-k-1F5K. Clones were verified by sequencing in both directions. All restriction enzymes were purchased from Takara or New England Biolabs. Taq polymerase (Promega) was used for all PCR. All enzymatic reactions were carried out using manufacturers' protocols.

### **Construction of antibody expression vectors**

Oligos LongT15fwd, LongT15rev, and PrimerB were used in a nested PCR similar to Horton<sup>25</sup> to construct a DNA sequence that encodes the T15 peptide. The resulting PCR product was cloned into the Sall-NotI sites in MCSB of pIRES (Clontech) to form pDXL. The complete heavy and light chains of pAc-k-1F5H and pAc-k-1F5K were PCR amplified using primers modVHXfwd and modVHXrev, or VKXfwd and VKXrev, respectively (Supplemental Figure 1). The light chain was cloned into the NheI-XhoI sites of MCSA of vector pDXL, and the heavy chain was cloned into the Sall-NotI sites of the resulting vector to form pch1F5 -DXL. Clones were verified by sequencing in both directions. To produce pch1F5 (anti-CD20 without the T15 peptide), pch1F5 -DXL and pIRES were digested with NotI and ClaI. Resulting DNA fragments of ~6 Kb from pch1F5-DXL, and ~2.2 Kb from pIRES were each gel purified from a 1% agarose gel using a Qiaquick kit (Qiagen), and ligated together to form pch1F5. Clones were verified by sequencing in both directions. All vector constructs were introduced into *E. coli* (XL-10 cells, from Stratagene) using the provided heat shock protocols. Plasmids were purified from 3 ml of overnight bacterial culture using a Qiagen mini-prep kit. Vectors pch1F5 and pch1F5 -DXL were electroporated into CHO-S cells using a 4 mm gap cuvette in an Eppendorf Multiporator set to 580 V and 40  $\mu$ s. Two days of recovery were allowed before the start of selection.

### **Purification of recombinant antibodies**

Cell culture supernatant was harvested every 3-5 days, depending on cell density. Cell suspensions were centrifuged at low speed (480-740 x g) for 7 to 10 minutes, and the supernatant was held at -20°C prior to additional processing. After rapid thawing at 37°C, supernatant was passed through a 0.2  $\mu$ m filter (Corning) by vacuum filtration to remove cell debris, and filtered supernatant was then passed over HiTrap Protein G HP column (GE Healthcare). Bound antibodies were eluted with 0.1 M glycine buffer pH 2.7, collected in 1mL fractions, and the pH was neutralized with 50  $\mu$ L 1M Tris pH 9. Elution profile was determined by reading UV absorbance at 280 (data not shown). Fractions with significant protein content were then pooled and concentrated using Amicon Ultra centrifugal filtration device 50,000 MW cutoff (Millipore) according to the manufacture's instructions.

### **Cell Surface Binding**

$3 \times 10^5$  per well of Raji, Ramos, or JOK-1 cells were seeded in a 24 well plate and incubated overnight at 37 °C and 5% CO<sub>2</sub>. Cells were then harvested and washed twice with PBS. Cells were resuspended in 1mL PBS and were incubated with either ch1F5 or DXL ch1F5 at

increasing concentrations (1  $\mu\text{g}$ , 5  $\mu\text{g}$ , 10  $\mu\text{g}$ , 20  $\mu\text{g}/\text{mL}$ ) and incubated at 4°C for 30 minutes. Excess antibody was removed by washing cells twice with PBS, and then cells were resuspended in a 1mL solution of FITC conjugated goat anti-Human (Sigma, 1:1000) and incubated at 4 °C for 30 minutes. After washing twice, cells were resuspended in 200 $\mu\text{L}$  PBS and analyzed by flow cytometry (BD FACSCalibur Instrument, BD Bioscience). Specific mean fluorescence intensity was determined by using the formula: specific MFI= MFI (primary Ab + goat anti-Human FITC) – MFI (goat anti-Human FITC).

### **Apoptosis Assay**

2x10<sup>5</sup> per well of Raji, Ramos, or JOK-1, cells were seeded in a 24 well plate and incubated overnight at 37 °C and 5% CO<sub>2</sub>. Cells were then treated with increasing concentrations of Abs for 20 hours at 37°C. Cells were harvested, washed once with PBS, and resuspended with 100  $\mu\text{L}$  1X annexin binding buffer containing 3 $\mu\text{L}$  annexin V Alexa Fluor 488 conjugate (Invitrogen) and propidium iodide (Sigma) at a final concentration of 4 $\mu\text{g}/\text{mL}$  to detect apoptosis and cell death, respectively. After 20 minutes incubation at 37 °C, cells were diluted with 150  $\mu\text{L}$  of 1X annexin binding buffer and analyzed by flow cytometry (BD FACSCalibur Instrument, BD Bioscience). Percent apoptotic cells was determined by gating the healthy population in the untreated control samples and using the formula: Percent Apoptotic Cells = (1-(Live Treated Target Cells/Live Untreated Target Cells)) \* 100.

### **CDC Assay**

2x10<sup>5</sup> cells were seeded into a 24 well plate and incubated overnight at 37 °C and 5% CO<sub>2</sub>. Cells were then treated with increasing concentrations of Abs for 2 hours at 37 °C in the presence of 5% rabbit HLA-ABC complement enriched sera (Sigma). Cells were harvested and washed once with PBS, resuspended in 200  $\mu\text{L}$  of PBS containing 50 nM calcein-AM (Biochemica) and 4  $\mu\text{g}/\text{mL}$  propidium iodide (Sigma). After incubation for 20 minutes at 37 °C cell viability was analyzed by flow cytometry (BD FACSCalibur Instrument, BD Bioscience). Percent killing was determined by the formula: Percent Dead Cells = (1-(Live Treated Target Cells/Live Untreated Target Cells)) \* 100.

### **PBMC Separation**

Peripheral blood mononuclear cells (PBMC) were prepared from healthy donors' buffy coat (Kentucky Blood Center, Lexington KY) by Ficoll-Hypaque density gradient centrifugation. PBMC were diluted to 6x10<sup>6</sup> cells/mL in hRPMI (10% FBS, low IgG) culture media and

maintained for a maximum of three days. PBMC viability and day- to-day cell population variation was analyzed by flow cytometry (BD FACSCalibur Instrument, BD Bioscience) before experimentation.

### **ADCC Assay**

Target cells (Raji, Ramos, or JOK-1) were harvested from T75 flasks and resuspended in 1mL of media containing 400 nM calcein-AM (Biochemica) and 8  $\mu$ L of TFL2 dye (OncoImmunin), used according to manufacturer's instructions. Target cells were labeled for 45 minutes at 37 °C, washed twice in media, and resuspended to a density of  $6 \times 10^5$  cells/mL. Effector cells (PBMC) were then harvested from T75 flasks and resuspended to a density of  $1.2 \times 10^7$  cells/mL. Target cells and effector cells were mixed at an E:T ratio of 20:1 then 250  $\mu$ L of cell mixture was aliquoted into individual 5mL round bottom tubes and incubated with increasing concentrations of Abs for 2 hours at 37°C. After incubation, target cell viability was analyzed by flow cytometry (BD FACSCalibur Instrument, BD Bioscience). Percent killing was determined by the formula: Percent Dead Cells =  $(1 - (\text{Live Treated Target Cells} / \text{Live Untreated Target Cells})) * 100$ .

## Results

### Construction of the ch1F5 and ch1F5-DXL antibodies

Several groups have demonstrated that cross-linking of therapeutic antibodies can improve the antibody's ability to kill target cells. These cross-linking methods include addition of secondary antibody, chemical cross-linking, and molecular engineering of multimeric forms<sup>13-17</sup>. We have previously shown that peptides can be photochemically added to affinity sites on antibodies<sup>20</sup>, and that photochemical addition of a specific peptide to antibodies can induce cross-linking *in situ*, what we term Dynamic Cross Linking (DXL)<sup>26</sup>. To further test the capacity of the DXL peptide, we have used molecular biological techniques to generate a chimeric version of the murine 1F5 antibody (ch1F5), and we have generated a chimeric DXL antibody that is identical to ch1F5, except for the addition of the DXL peptide to the C-terminus of each heavy chain. Figure 1 shows a drawing of the structures of ch1F5 and ch1F5-DXL.

### Binding to human B-cell lines using FACS

To verify that the recombinant ch1F5 and ch1F5-DXL antibodies are functional, we tested their ability to bind to cells from the human B-cell JOK-1 line, using fluorescence activated cell sorting (FACS). In Figure 2, the dotted line shows the mean fluorescence intensity (MFI) of staining with the ch1F5-DXL antibody, while the solid line represents the staining using the ch1F5, non-DXL antibody. Binding of the ch1F5-DXL antibody was approximately four-fold higher than binding of ch1F5.

### Induction of Apoptosis is dependent on receptor cross-linking

One of the proposed mechanisms of DXL antibodies is receptor crosslinked induction of apoptosis<sup>16,17</sup>. We compared the induction of apoptosis of the ch1F5 and DXL antibodies in three cell lines Raji, Ramos and JOK-1. As seen in Figure 3, addition of 20 µg of ch1F5 induces apoptosis in approximately 30% of the cells (Figure 3B versus Figure 3A). The DXL antibody induces significantly more apoptosis than the naked chimeric (Figure 3C versus Figure 3B). Similarly, the DXL antibody is a more potent inducer of apoptosis in Ramos cells at a concentration of 10 µg (Figure 3F versus Figure 3D-E). In Table 1 we show the apoptotic effects of the two antibodies over a range of concentrations. It is interesting to note, at lower concentration of Abs the enhancing effect is much more pronounced. For example, after

treatment of Raji cells with 5 $\mu$ g/mL of either antibody, the percent of apoptotic cells is 2.5 fold higher after DXL treatment, but it is slightly less than 2-fold higher after treatment with 20  $\mu$ g/mL.

### **Comparison of Complement Dependent Cytotoxicity**

Next, we compared the CDC activity of the ch1F5 and ch1F5-DXL. CDC is induced after binding of complement components to the Fc region of an antibody, and is potent in the IgG1 isotype, which is the isotype of the DXL construct. An enhancing effect was observed in all cell lines. As seen in Figure 4A, for example, at 5  $\mu$ g /mL there was virtually no CDC activity in Raji cells with the chimeric, however, 35% of cells were killed with the DXL Ab. This correlates to the highest improvement of effectiveness in apoptosis. It is interesting to note that the potency of the DXL antibody plateaus at 5  $\mu$ g /ml in Ramos cells (Figure 4B). The ch1F5 appears to plateau at 10  $\mu$ g /ml, but it does not reach the potency of the DXL Ab at any level tested, suggesting that even higher doses would not reach the killing capacity of 5  $\mu$ g /ml DXL Ab.

### **Comparison of ADCC**

Since Type I antibodies, such as the murine 1F5, do not induce high levels of ADCC activity<sup>27</sup>, it was interesting to test the chimeric antibody in its ability to induce ADCC. As shown in Figure 5A-B, the DXL antibody induces significantly more ADCC than ch1F5 in Raji and Ramos cells at 1  $\mu$ g /ml and 3  $\mu$ g /ml, but the increase in potency is not significant at 7.5  $\mu$ g /ml.

### **Inhibition of Lymphoma Growth *In Vitro***

To approximate the *in vivo* killing potential of these anti-CD20 antibodies on tumor cells, we tested the anti-proliferative effects of the ch1F5 and ch1F5-DXL in Raji and Ramos cell lines. The assay measures the level of fluorescence dye binding to nucleic acid (Methods and Materials). As shown in Figure 6A-B, the DXL antibody inhibited proliferation to a greater extent in both cell lines at all concentrations tested.

## Discussion

Strategies to improve immunotherapy include increasing the affinity for target, increasing Complement-Dependent Cytotoxicity and Antibody-Dependent Cell-mediated Cytotoxicity<sup>28</sup>. Therapeutic antibodies have limitations with regard to patient population and disease variants. For example, Herceptin™, an anti-Her2 antibody, is effective in only 25% of breast cancer patients due to low expression of the Her2/neu target<sup>29</sup>. Rituxan™, a chimeric anti-CD20 antibody, induces a high initial response in non-Hodgkin's lymphoma and follicular lymphoma patients, but many patients eventually relapse<sup>30</sup>. To overcome these limitations, Vitetta and coworkers chemically cross-linked anti-CD19 and anti-CD20 antibodies, creating chemical homo-dimers and improved tumor killing *in vitro* and in xenografts mouse models<sup>13</sup>. Potency increase can also be achieved *in vitro* with a secondary antibody against the primary antibody to facilitate cross-linking<sup>12</sup>.

We have developed an alternative strategy to chemical antibody homo-dimers or to the use of secondary antibodies to induce tumor target cross-linking, taking advantage of a homo-dimerizing domain in a rare class of antibody<sup>18,21,23,31</sup>. This antibody contains a domain which induces dimerization upon docking to its specific target but remains monomeric in solution<sup>16</sup>. As previously reported, a 24mer peptide, corresponding to this domain plus a linker was affinity photo-linked to antibodies. These antibody conjugates induce enhanced effector functions *in vitro*<sup>16,17,26</sup> and *in vivo* (M.R. and H.K., unpublished results).

In contrast to the chemically cross-linked antibody dimers which are limited by the density of antigen targets, facultative homo-dimerizing or self-binding antibodies have the ability through lattice formation to cross-link low density receptors. In addition, they can form, via self-binding, additional lattices covering the first layer of antigen-bound antibodies. The proposed mode of action of these antibodies is to induce lattice formation on target and increase receptor movement into lipid rafts, which is the initial step of signaling pathways. Facultative homodimerizing antibodies are in equilibrium between monomeric and dimeric states, whereby in physiological conditions the monomer is dominant in solution<sup>16</sup>. Upon docking to target, the equilibrium shifts to the dimer state. The term Dynamic Cross Linking (DXL) describes this mechanism. DXL antibodies increase potency with respect to targeting, effector functions, apoptosis, and animal models<sup>16,17,26</sup>

In this report we describe the generation of DXL antibody against CD20 as a recombinant fusion protein. For this construct we have chosen the C-terminus as the attachment point for the homodimerizing domain, and we have shown the improved potency of the resulting DXL antibody. The DXL version of the chimeric 1F5-derived antibody provides significant improvements in effector functions and apoptosis, across multiple cell lines, versus the chimeric, non-DXL antibody.

Figure 1 illustrates the placement of the T15 homophilic domain in the chimeric structure. The C-terminal attachment point assures that the homodimerizing domain does not interfere with target or complement binding, however, it may not provide optimal increase in potency. We are currently developing other constructs in which the homodimerizing domain is attached to the antibody of interest at different locations, to allow direct comparison of the effect of positioning on DXL effectiveness.

Anti-CD20 antibodies differ greatly in their potency when tested *in vitro* using different cell lines and assays<sup>32,33</sup>. Using CDC as criteria Glennie et al<sup>27</sup> divided different anti-CD20 antibodies into two types. Type I anti-CD20 activates complement efficiently, while type II mediates ADCC not CDC. The 1F5 anti-CD20 belongs together with Rituxan to the type I class. Even though the parental 1F5 anti-CD20 belongs to the type I class, the DXL version shows a significant increase of ADCC activity, therefore gaining type II properties. This creates a new class of therapeutic antibodies, designated here as type III.

C1q binding correlates with the amount and spacing of Fc on the target cell. Our model of DXL binding proposes lattice formation on targets, and two possible mechanisms for increased CDC. Lattice formation increases the total level of Fc available for C1q binding. In addition, the self-binding property tethers the antibodies on the cell surface into a conformation that promotes optimal spacing, which was shown to drastically enhance CDC, via C1q binding<sup>34</sup>.

Similarly, the DXL anti-CD20 increases the amount of apoptosis twofold over the “naked” anti-CD20. This agrees with the proposed mode of action in apoptosis signaling to move the antibody into lipid rafts enhanced by cross-linking<sup>35</sup>. Since *in vitro* assays of antibody potency can be unreliable predictors of patient’s response, animal models using xenografts are needed to gain further confidence to initiate clinical trials with DXL antibodies.

The present report provides a blueprint for making recombinant DXL antibodies with enhanced potency as demonstrated with the chemical DXL antibody conjugate<sup>16,17,26</sup>. This sets the stage for large-scale production of recombinant DXL antibodies using industry standard techniques.

## **Acknowledgments**

This work was supported by funding from Innexus Biotechnology, Inc., 13208 E. Shea Blvd. MCCRБ #200, Scottsdale AZ, 85259.

The authors wish to thank Xiaoping Wu for cell culture of Ramos, Raji, and JOK-1 cell lines.

## **Authorship**

Contributions: HK directed the research. JDA designed all recombinant DNA constructs, and performed research. KR performed research, collected data, and analyzed and interpreted data. MR analyzed and interpreted data. HK, JDA, KR and MR all drafted portions of the manuscript.

Conflict of interest disclosures: 1. The authors (HK, JDA, KR, MR) are employed by Innexus Biotechnology, Inc., whose potential product was studied in the present work. 2. HK and JDA are authors on a pending patent related to the work that is described in the present study.

Correspondence: Heinz Kohler, Innexus Biotechnology, Inc., 1501 Bull Lea Rd., Lexington, KY 40511; email: [hkohler@ixsbio.com](mailto:hkohler@ixsbio.com).

## References

1. Ho M, Kreitman RJ, Onda M, Pastan I. In vitro antibody evolution targeting germline hot spots to increase activity of an anti-CD22 immunotoxin. *J Biol Chem*. 2005;280:607-617.
2. Nechansky A, Schuster M, Jost W, et al. Compensation of endogenous IgG mediated inhibition of antibody-dependent cellular cytotoxicity by glyco-engineering of therapeutic antibodies. *Mol Immunol*. 2007;44:1815-1817.
3. Schuster M, Umana P, Ferrara C, et al. Improved effector functions of a therapeutic monoclonal Lewis Y-specific antibody by glycoform engineering. *Cancer Res*. 2005;65:7934-7941.
4. Scallon B, McCarthy S, Radewonuk J, et al. Quantitative in vivo comparisons of the Fcγ receptor-dependent agonist activities of different fucosylation variants of an immunoglobulin G antibody. *Int Immunopharmacol*. 2007;7:761-772.
5. Scallon BJ, Tam SH, McCarthy SG, Cai AN, Raju TS. Higher levels of sialylated Fc glycans in immunoglobulin G molecules can adversely impact functionality. *Mol Immunol*. 2007;44:1524-1534.
6. Foote J, Eisen HN. Breaking the affinity ceiling for antibodies and T cell receptors. *Proc Natl Acad Sci U S A*. 2000;97:10679-10681.
7. Foote J, Eisen HN. Kinetic and affinity limits on antibodies produced during immune responses. *Proc Natl Acad Sci U S A*. 1995;92:1254-1256.
8. Rathanaswami P, Roalstad S, Roskos L, Su QJ, Lackie S, Babcook J. Demonstration of an in vivo generated sub-picomolar affinity fully human monoclonal antibody to interleukin-8. *Biochem Biophys Res Commun*. 2005;334:1004-1013.
9. Jain RK. Physiological barriers to delivery of monoclonal antibodies and other macromolecules in tumors. *Cancer Res*. 1990;50:814s-819s.
10. Kelley RF, O'Connell MP, Carter P, et al. Antigen binding thermodynamics and antiproliferative effects of chimeric and humanized anti-p185HER2 antibody Fab fragments. *Biochemistry*. 1992;31:5434-5441.
11. Shan D, Ledbetter JA, Press OW. Signaling events involved in anti-CD20-induced apoptosis of malignant human B cells. *Cancer Immunol Immunother*. 2000;48:673-683.
12. Shan D, Ledbetter JA, Press OW. Apoptosis of malignant human B cells by ligation of CD20 with monoclonal antibodies. *Blood*. 1998;91:1644-1652.
13. Ghetie MA, Podar EM, Ilgen A, Gordon BE, Uhr JW, Vitetta ES. Homodimerization of tumor-reactive monoclonal antibodies markedly increases their ability to induce growth arrest or apoptosis of tumor cells. *Proc Natl Acad Sci U S A*. 1997;94:7509-7514.
14. Zhang N, Khawli LA, Hu P, Epstein AL. Generation of rituximab polymer may cause hyper-cross-linking-induced apoptosis in non-Hodgkin's lymphomas. *Clin Cancer Res*. 2005;11:5971-5980.
15. Ghetie MA, Bright H, Vitetta ES. Homodimers but not monomers of Rituxan (chimeric anti-CD20) induce apoptosis in human B-lymphoma cells and synergize with a chemotherapeutic agent and an immunotoxin. *Blood*. 2001;97:1392-1398.
16. Zhao Y, Kohler H. Enhancing tumor targeting and apoptosis using noncovalent antibody homodimers. *J Immunother*. 2002;25:396-404.
17. Zhao Y, Lou D, Burke J, Kohler H. Enhanced anti-B-cell tumor effects with anti-CD20 superantibody. *J Immunother*. 2002;25:57-62.

18. Kaveri SV, Halpern R, Kang CY, Kohler H. Self-binding antibodies (autobodies) form specific complexes in solution. *J Immunol.* 1990;145:2533-2538.
19. Miller K, Meng G, Liu J, et al. Design, construction, and in vitro analyses of multivalent antibodies. *J Immunol.* 2003;170:4854-4861.
20. Russ M, Lou D, Kohler H. Photo-activated affinity-site cross-linking of antibodies using tryptophan containing peptides. *J Immunol Methods.* 2005;304:100-106.
21. Kang CY, Brunck TK, Kieber-Emmons T, Blalock JE, Kohler H. Inhibition of self-binding antibodies (autobodies) by a VH-derived peptide. *Science.* 1988;240:1034-1036.
22. Kaveri SV, Kang CY, Kohler H. Natural mouse and human antibodies bind to a peptide derived from a germline VH chain. Evidence for evolutionary conserved self-binding locus. *J Immunol.* 1990;145:4207-4213.
23. Halpern R, Kaveri SV, Kohler H. Human anti-phosphorylcholine antibodies share idiotopes and are self-binding. *J Clin Invest.* 1991;88:476-482.
24. Anderson KC, Bates MP, Slaughenhaupt BL, Pinkus GS, Schlossman SF, Nadler LM. Expression of human B cell-associated antigens on leukemias and lymphomas: a model of human B cell differentiation. *Blood.* 1984;63:1424-1433.
25. Horton RM. PCR-mediated recombination and mutagenesis. SOEing together tailor-made genes. *Mol Biotechnol.* 1995;3:93-99.
26. Zhao Y, Russ M, Retter M, et al. Endowing self-binding feature restores the activities of a loss-of-function chimerized anti-GM2 antibody. *Cancer Immunol Immunother.* 2007;56:147-154.
27. Cragg MS, Glennie MJ. Antibody specificity controls in vivo effector mechanisms of anti-CD20 reagents. *Blood.* 2004;103:2738-2743.
28. Schaedel O, Reiter Y. Antibodies and their fragments as anti-cancer agents. *Curr Pharm Des.* 2006;12:363-378.
29. Gonzalez-Angulo AM, Hortobagyi GN, Esteva FJ. Adjuvant therapy with trastuzumab for HER-2/neu-positive breast cancer. *Oncologist.* 2006;11:857-867.
30. Marcus R, Hagenbeek A. The therapeutic use of rituximab in non-Hodgkin's lymphoma. *Eur J Haematol Suppl.* 2007;5-14.
31. Kang CY, Cheng HL, Rudikoff S, Kohler H. Idiotypic self binding of a dominant germline idio type (T15). Antibody activity is affected by antibody valency. *J Exp Med.* 1987;165:1332-1343.
32. Chan HT, Hughes D, French RR, et al. CD20-induced lymphoma cell death is independent of both caspases and its redistribution into triton X-100 insoluble membrane rafts. *Cancer Res.* 2003;63:5480-5489.
33. Cardarelli PM, Quinn M, Buckman D, et al. Binding to CD20 by anti-B1 antibody or F(ab')(2) is sufficient for induction of apoptosis in B-cell lines. *Cancer Immunol Immunother.* 2002;51:15-24.
34. Introna M, Golay J. Mechanism of action of therapeutic monoclonal antibodies. *Hematology (EHA Educ Program).* 2005;1:161-165.
35. Cragg MS, Morgan SM, Chan HT, et al. Complement-mediated lysis by anti-CD20 mAb correlates with segregation into lipid rafts. *Blood.* 2003;101:1045-1052.

**Table 1. Induction of Apoptosis**

<b>Cell line</b>	<b>Antibody/ml<sup>1</sup></b>	<b>ch1F5<sup>2</sup></b>	<b>DXL-ch1F5<sup>3</sup></b>
Raji			
	1µg	0.83±2.18	5.06±2.16
	5µg	14.90±1.81	36.91±8.73
	10µg	26.73±4.28	47.40±2.89
	20µg	30.05±3.13	58.37±4.67
Ramos			
	1µg	4.00±0.11	19.36±2.06
	5µg	20.11±2.30	33.06±7.10
	10µg	24.61±0.40	42.53±4.28
	20µg	31.74±1.70	40.79±1.41
Jok-1			
	1µg	7.85±0.99	4.39±0.99
	5µg	23.77±5.48	27.19±12.14
	10µg	59.43±13.89	52.12±18.97
	20µg	49.44±7.50	56.87±4.60

<sup>1</sup> Differing amounts of antibodies were added for 20 hours to each cell line

<sup>2</sup> Percent apoptotic cells induced by ch1F5

<sup>3</sup> Percent apoptotic cells induced by DXL-ch1F5

**Figure legends:**

**Figure 1: Structures of the chimeric 1F5 (ch1F5) and DXL 1F5 (ch1F5 –DXL) antibodies.**

**Figure 2: Comparison of binding of ch1F5 to DXL-ch1F5 to JOK-1 cells using FACS on fixed cells.**

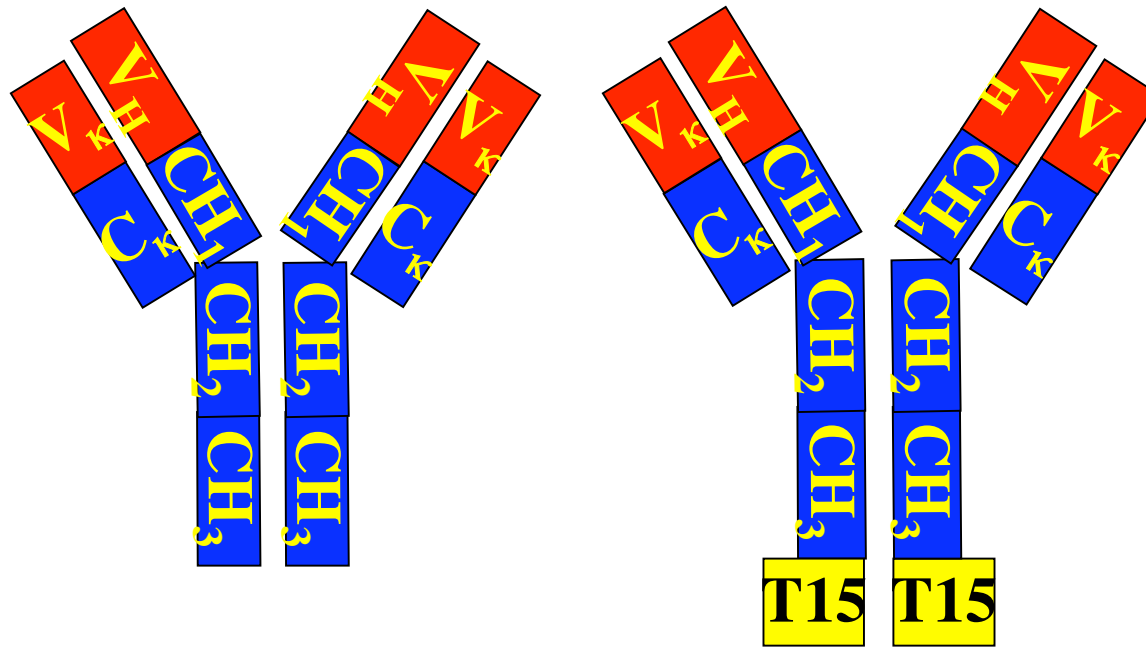
**Figure 3: Comparison of induction of apoptosis by ch1F5 and DXL-ch1F5 on Raji (A-C) and Ramos (D-F) cells. Panels A and D cells only, B and E ch1F5, C and F DXL-ch1F5.**

**Figure 4: Comparison of CDC using ch1F5 and DXL-ch1F5. Panel A, Raji, B, Ramos, C, JOK-1.**

**Figure 5: Comparison of ADCC using ch1F5 and DXL-ch1F5. Panel A, Raji, B, Ramos.**

**Figure 6: Comparison of inhibition of proliferation, Panel A, Raji, B, Ramos, with ch1F5 and DXL-ch1F5.**

Figure 1



Chimeric 1F5

Chimeric DXL-1F5

Figure 2

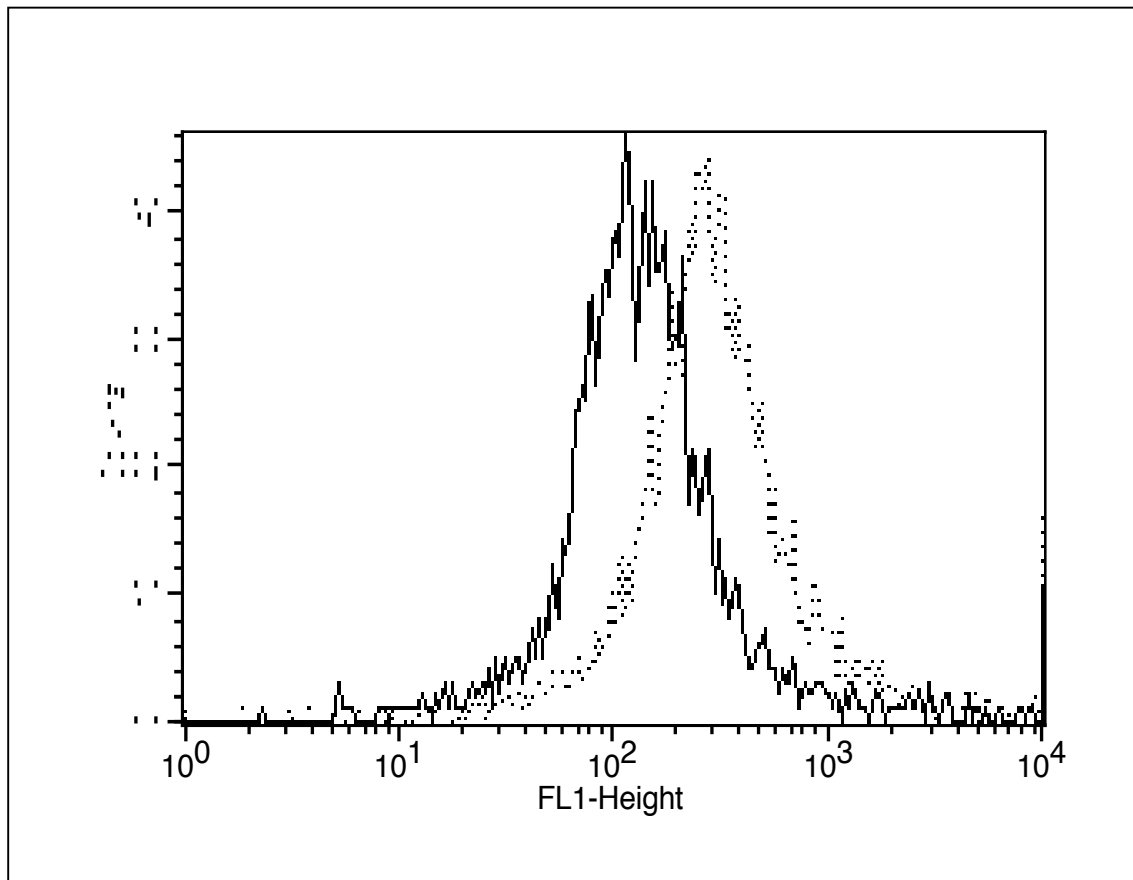
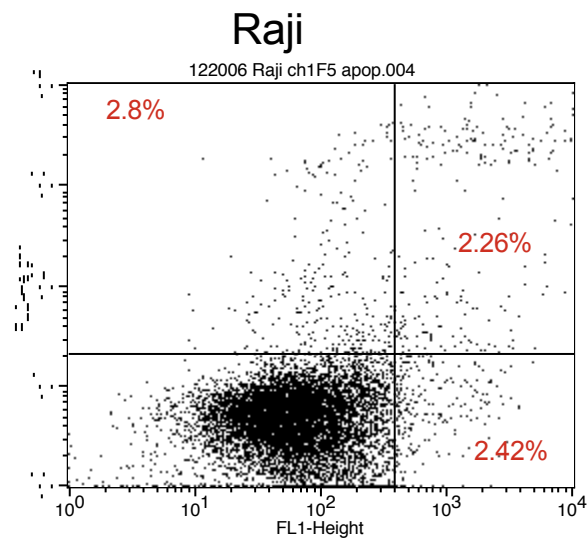
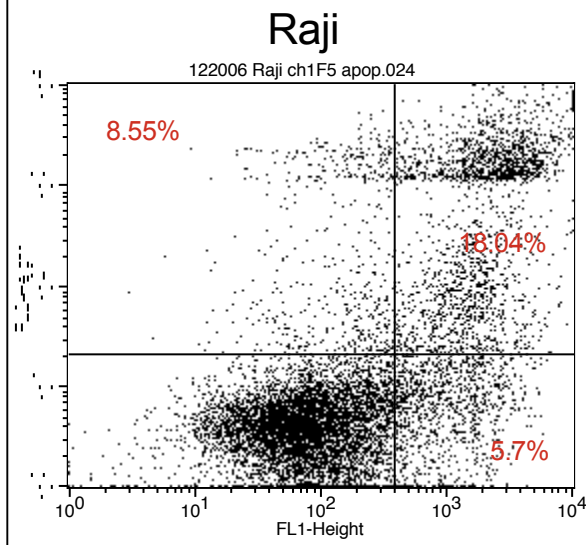


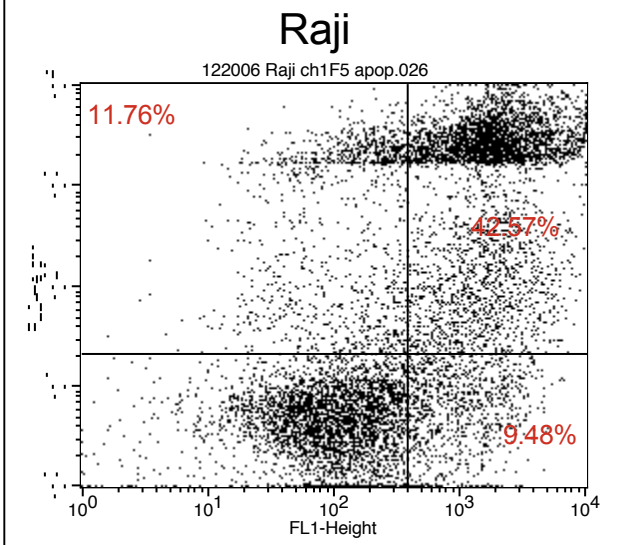
Figure 3



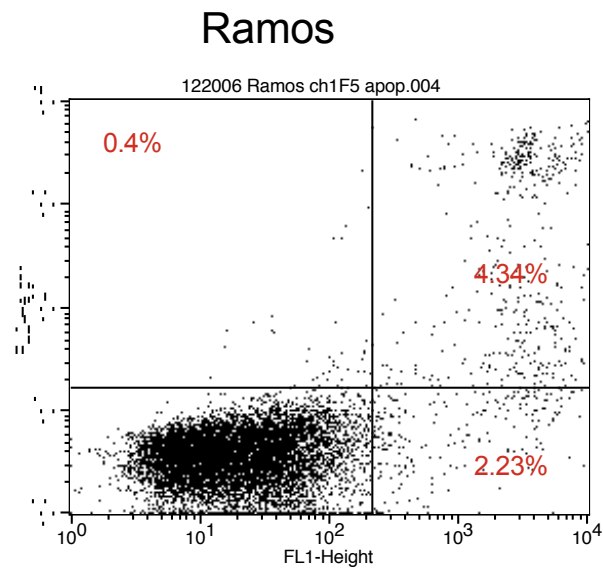
**A**



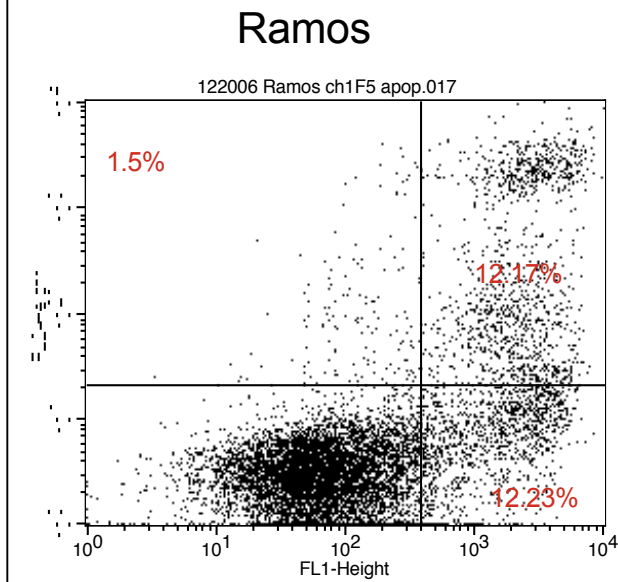
**B**



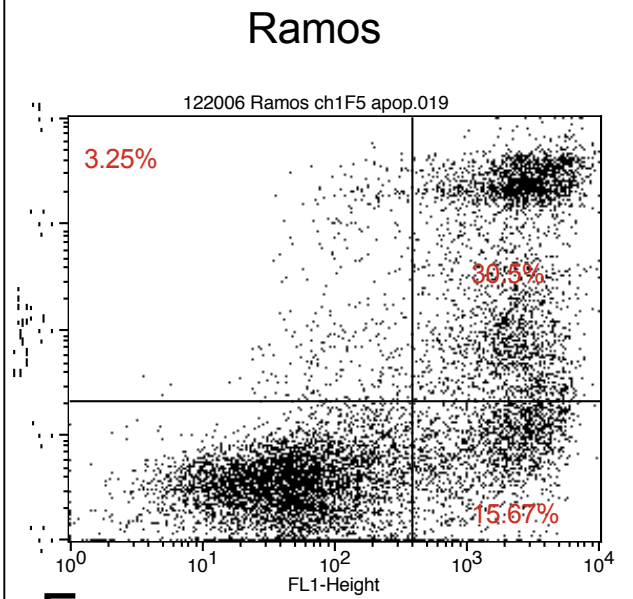
**C**



**D**

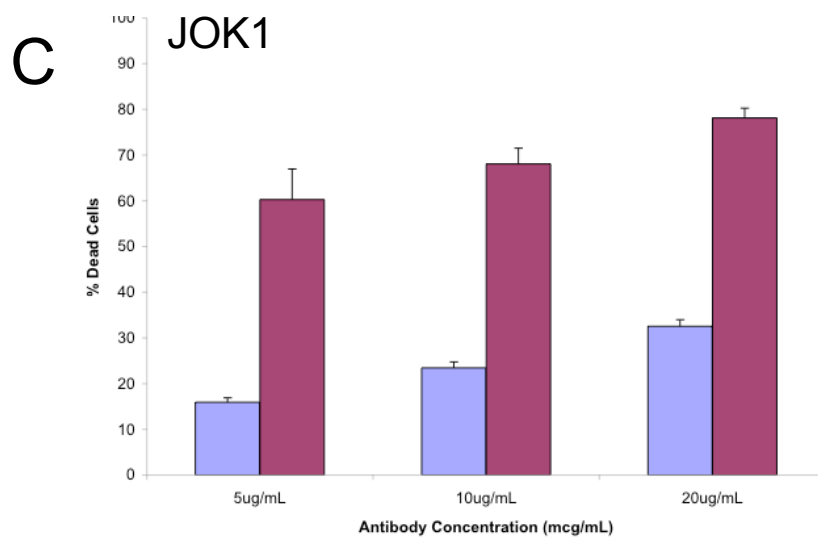
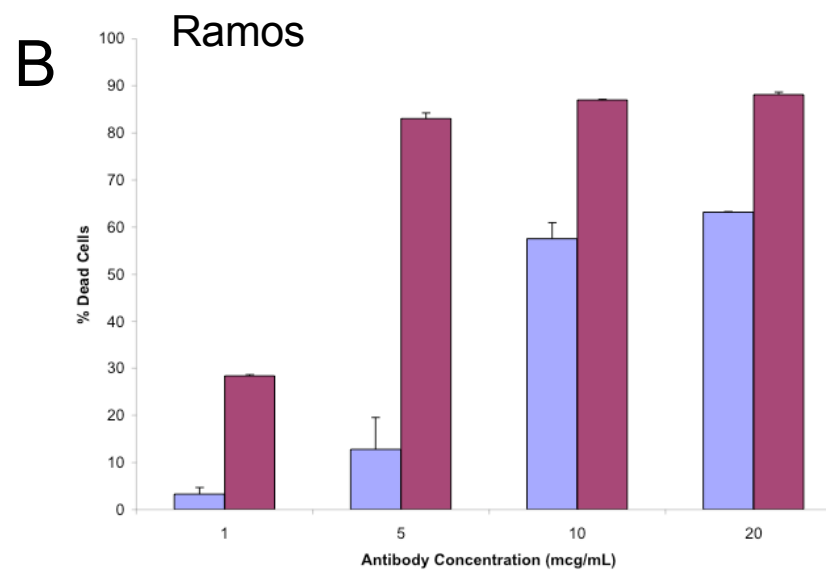
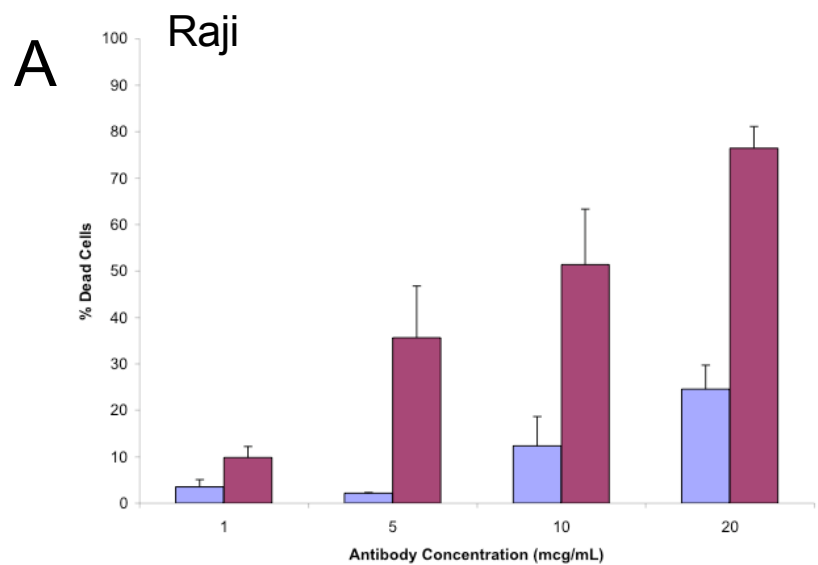


**E**



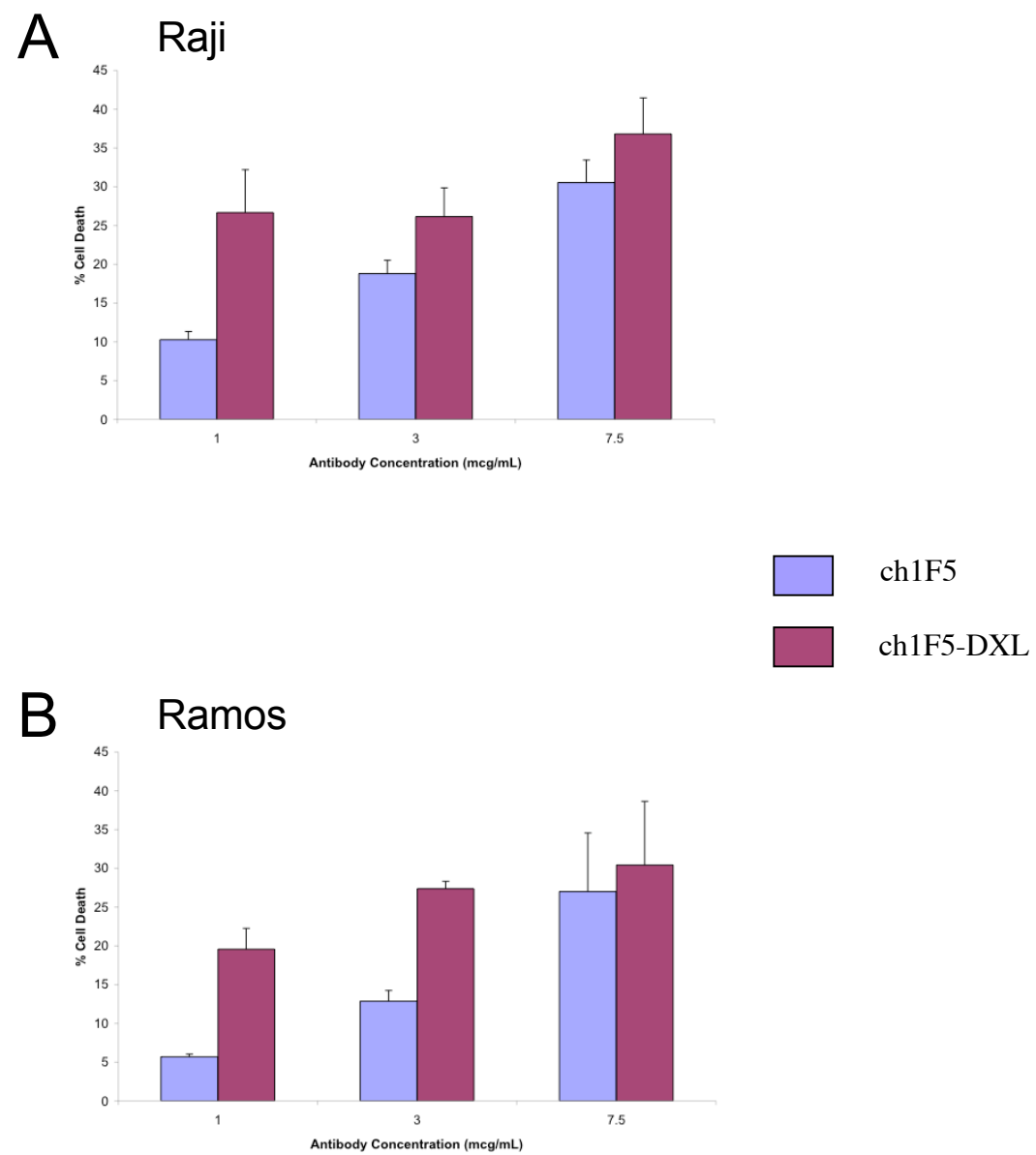
**F**

Figure 4



ch1F5  
ch1F5-DXL

Figure 5



**A**

**Raji**

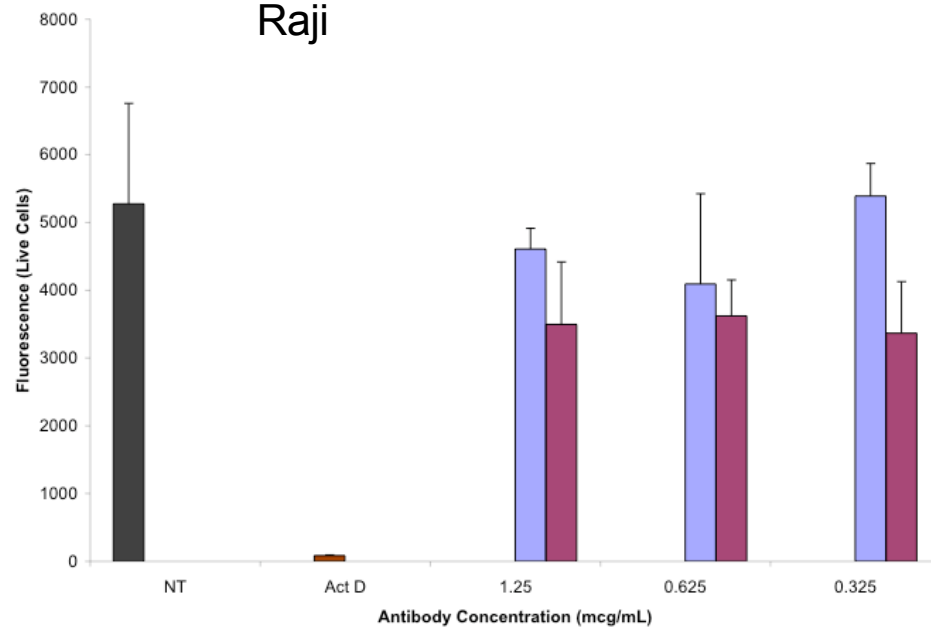
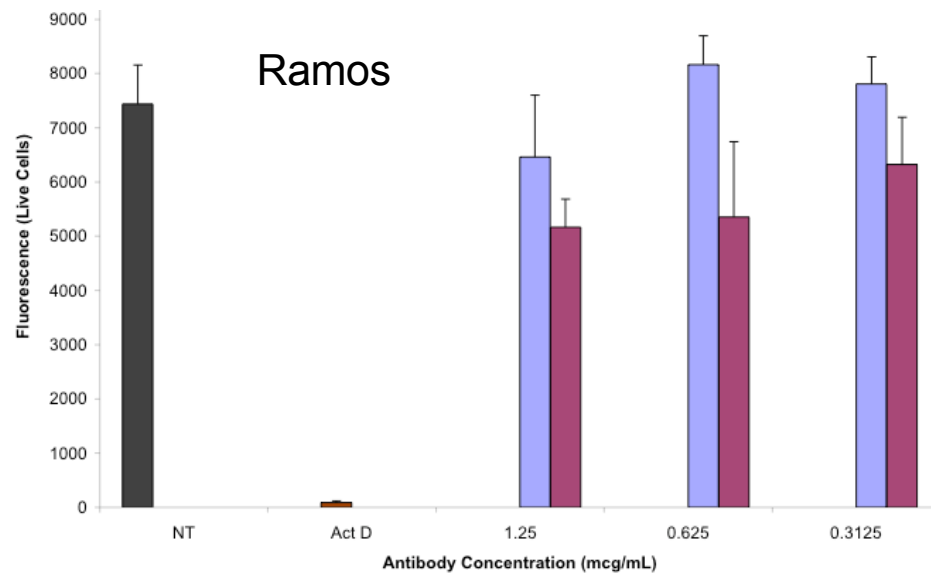


Figure 6

**B**

**Ramos**



ch1F5  
ch1F5-DXL